IEEE Access
Multidisciplinary | Rapid Review | Open Access Journal

Received 23 April 2024, accepted 13 May 2024, date of publication 15 May 2024, date of current version 28 May 2024.

Digital Object Identifier 10.1109/ACCESS.2024.3401243

RESEARCH ARTICLE

Microwave Power Limiter Having H-Shaped Slot Structure With Enhanced Plasma Discharge by Electrostatic Potential

KYOUNG-JE PARK[1,2], JAE-HYUN PARK[1], WANG-SANG LEE[2], (Senior Member, IEEE), AND JEONG-MIN WOO[3]

[1]I-SPEC, Uichang-gu, Changwon-si, Gyeongsangnam-do 51395, South Korea
[2]Gyeongsang National University, Jinju-si, Gyeongsangnam-do 52828, South Korea
[3]Korea Electrotechnology Research Institute, Seongsan-gu, Changwon-si, Gyeongsangnam-do 51543, South Korea

Corresponding author: Jeong-Min Woo (woojm@keri.re.kr)

This work was supported in part by Korea Research Institute for Defense Technology Planning and Advancement (KRIT) grant funded by the Defense Acquisition Program Administration (DAPA), South Korea, under Grant KRIT-CT-21-038; and in part by the Private Research Program conducted by Korea Electric Research Institute with the support of Korea Research Institute for Defense Technology Planning and Advancement (KRIT) grant funded by the Defense Acquisition Program Administration (DAPA), South Korea, under Grant 22A03028.

ABSTRACT A microwave power limiter with an H-type slot structure is proposed as a waveguide structure that blocks high-power microwaves through plasma discharge. At an operating frequency of 5.75 GHz, the electric field is concentrated in the discharging electrode gap; when high power is applied, the plasma limiter discharges, and low power is transmitted. By contrast, when low power is applied, it is transmitted without loss. An H-type resonance structure was used to increase the electric field concentration and selectivity within the waveguide. At 5.75 GHz, the insertion loss of the H-type slot structure was 1.85 dB. The electric field concentration increased to 49492 V/m, and the 3 dB bandwidth was 535 MHz. In addition, the plasma discharge onset level in the xenon gas was lower because of the electrostatic potential. When an electrostatic potential of 300 V was applied, the plasma discharge onset level decreased from 310 to 180 W.

INDEX TERMS Plasma limiter, waveguide, microwave, electrostatic potential.

I. INTRODUCTION

Microwave technology plays an important role in a wide range of applications, and is used in various fields, such as communications, radio detection and ranging (RADAR), and medicine [1], [2], [3]. RADAR has recently been used extensively in the military and aerospace fields [4], [5]. RADAR systems operate using microwave devices and circuits [6], [7]. However, various threats have led to an unstable operation of RADAR systems. Among the various threats, electromagnetic pulses (EMPs) are a type of emission phenomenon with high-power electromagnetic fields and electromagnetic energy typically more than 1 kW, and are electromagnetic waves in the form of an impulse with a wide frequency spectrum from MHz to GHz. EMPs are generally caused by nuclear explosions, lightning, or certain electromagnetic-field-generating devices [8], [9], [10], [11], [12]. The EMP changes rapidly in electromagnetic waves, and is attracting particular attention from a military perspective owing to its irregular and sudden phenomena [13]. EMPs have a fast rise time less than ns, and these characteristics pose a significant threat to the safety of electromagnetic devices.

The associate editor coordinating the review of this manuscript and approving it for publication was Mohamed Kheir.

A low-noise amplifier (LNA) is one of the most important components of a RADAR system. LNAs amplify very weak signals received from the RADAR antenna. Therefore, they have a significant influence on the performance of RADAR systems, and are likely to be affected by high-power and strong signals, such as EMP threats [14], [15], [16]. These high-power signals can generate unnecessary voltages inside the device, which can lead to poor performance or destruction of the device [17], [18].

To minimize the influence of EMPs on RADAR systems, EMP preparedness measures must be considered during the design and configuration stages of RADAR systems, including the LNA. It is important to protect the LNA by applying EMP-blocking devices and protection devices. Additionally, to improve the durability of the LNA, it is necessary to avoid using EMP-sensitive parts and to prepare countermeasures for quick recovery when an EMP occurs.

To protect the LNA of a RADAR system, a diode element is installed at the LNA stage, or a diode-integrated EMP protection device is used in front of the LNA [19], [20], [21]. The diode limiter controls and disperses the EMP using diode breakdown to reduce the energy transmitted to the LNA. A diode element in an EMP protection device operates as a limiter that transmits energy when low-power electromagnetic waves are incident and suppresses energy when high-power electromagnetic waves are incident. In addition, the diode limiter has a frequency-shift function that helps protect the LNA by moving the EMP out of the frequency range of the LNA or bypassing unwanted signals to the ground. Recently, a plasma-discharge slot structure has been adopted to limit the EMP and reduce the energy transmitted to the LNA [22]. It has the advantage of a high power capacity of more than 10 kW, whereas the diode limiter has a power capacity of only 10 W [19]. Depending on the specific design of the plasma limiter, the plasma discharge is enhanced to prevent the EMPs from directly reaching the LNA. However, the plasma limiter responds to the EMP when the magnitude of the incident pulse is approximately 200 W or higher, whereas the LNA receives a magnitude in microwatts [23]. Various gas types and pressures have been adopted to reduce the response power of plasma limiters [24], [25].

In this study, the plasma discharge of a microwave power limiter based on waveguide was enhanced by the electrostatic potential at the discharging electrode. Previous studies have only focused on waveguide devices that react when an EMP is incident, and the results of applying an electric bias to a plasma limiter have not yet been reported. In addition, various types of resonant slot structures enhance plasma discharge. Straight and H-shaped slot structures have been proposed [26], [27]. The straight slot structure has the advantage of being easy to design and manufacture, but has the disadvantage of difficulty in achieving high efficiency in the limited space of the waveguide. Thus, an H-shaped slot structure is employed. The insertion loss of the normal signal is similar to that of the existing straight type, but it has the advantage of a higher electric-field concentration to enhance plasma discharge.

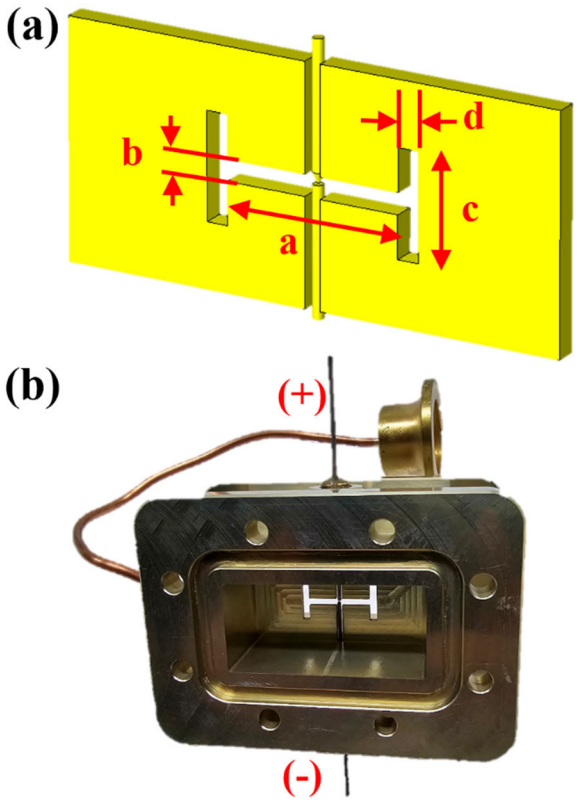

FIGURE 1. (a) Schematic and (b) demonstrated power limiter.

TABLE 1. Design parameter of power limiter.

Parameter	A	B	C	D
Value (mm)	16.5	2	10	2

II. DESIGN OF THE MICROWAVE POWER LIMITER

The microwave power limiter should exhibit low insertion loss characteristics for normal signals with low incident power and high insertion loss for transient signals. Figure 1 shows a schematic of the power limiter based on the WR 187 standard waveguide structure. The power limiter was fabricated using the dip-brazing method, and the discharging electrode with a diameter of 1 mm was made of tungsten. The gas line and viewport were located separately on the sidewall. An H-shaped slot structure was designed; its main parameters are shown in Fig. 1(a). The discharging electrodes were located across the slot structure and electrically isolated from the body of the power limiter to bias the voltage. The gap distance between the upper and lower discharging electrodes was 100 μm.

An analysis of the design parameters in Fig. 1(a) is shown in Fig. 2. Electromagnetic simulations were conducted

using commercial software (CST). The waveguide port was located in front of the waveguide model, and the probe was located at the back of the waveguide. The electromagnetic boundary condition was to have an open boundary at outside of the waveguide. Parameters A and B were analyzed in a previous report in which the resonant frequency shifted to a higher frequency band as the parameters decreased [28]. These parameters include the LC resonance, which results in bandpass characteristics. The analysis of the H-shaped side wings showed a similar tendency. As parameters C and D decreased, the resonant frequency shifted to a higher frequency band. The optimized design parameters are shown in Table 1. The target resonant frequency was 5.75 GHz.

The electric field distribution was simulated, as shown in Fig. 3. Straight and H-shaped slot structures were compared with same input power, and both structures were designed with a resonant frequency of 5.75 GHz. As shown in Fig. 3(a), the maximum electric field of the straight slot structure was 40939 V/m, and was located at the discharge electrode gap. The maximum electric field of the H-shaped slot structure was 49492 V/m at the discharge electrode gap, which is 20% higher than that of the straight slot structure. The concentrated electric field distribution of H-shaped slot structure is expected to discharge at a lower incident power compared with the straight slot structure.

The normal signal transfer characteristics of the straight and H-shaped slot structures are compared in Fig. 4. Both the structures exhibited a resonant frequency of 5.75 GHz. The insertion losses of the straight and H-shape slot structures were calculated as 0.12 and 0.13 dB, respectively. The 3 dB bandwidths of the straight and H-shaped slot structures were 952 and 708 MHz, respectively. The H-shaped slot structure showed a higher selectivity for the bandpass filter characteristics. The transfer characteristics of the H-shaped slot structure were verified using a network analyzer. The insertion loss of the demonstrated power limiter was 1.85 dB at 5.75 GHz, and the 3 dB bandwidth was 535 MHz.

The pre-ionization in electrostatic field was performed to verify the enhance of the plasma discharge [29]. The electrostatic potential and field distribution were calculated using commercial software (CST) to verify the effect of the electrostatic potential on the discharging electrode. An electrostatic model was adopted, and the boundary conditions were set as open boundaries in each direction. As shown in Fig. 5(a), the electrostatic potential was set to 300 V at the upper discharge electrode. The electrostatic field distribution is shown in Fig. 5(b). The air breakdown voltage of the electrostatic electrodes was reported to be 3000 kV/m [30]. The maximum electrostatic field was calculated to be 657 kV/m at the gap between the discharging electrodes, and the maximum electrostatic field value increased linearly as the electrostatic potential increased. The value of the maximum electrostatic field in a power limiter model has been decreased compared

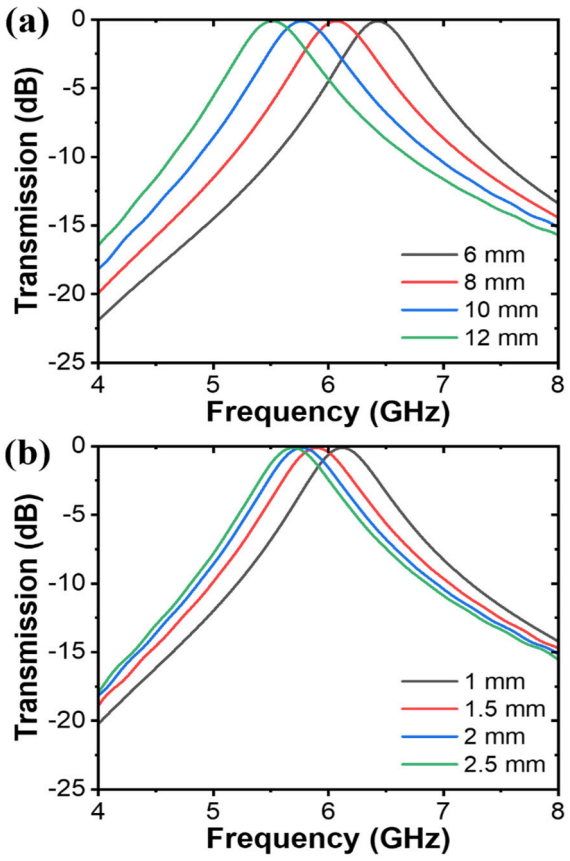

FIGURE 2. Simulation results of the H-shaped slot structure; Sweeping of (a) parameter C, (b) parameter D.

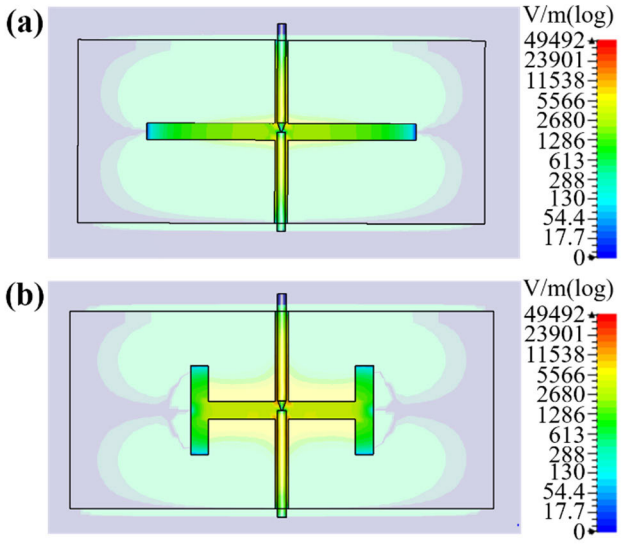

FIGURE 3. Simulated electric field distribution; (a) Straight slot structure, (b) H-shape slot structure.

with that of an ideal plate-to-plate model where the plate-to-plate distance is 100 μm. The surrounding waveguide

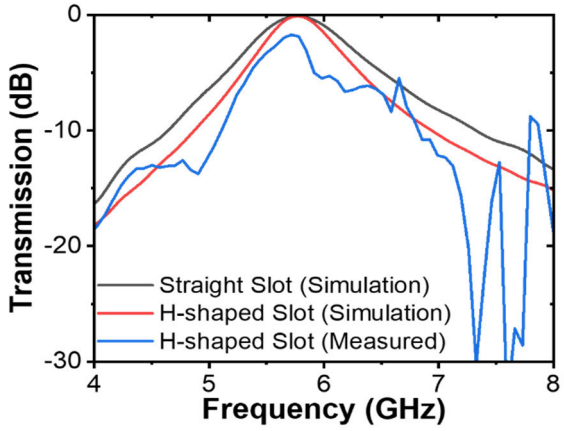

FIGURE 4. Simulation and transmission measurement results of the microwave power limiter.

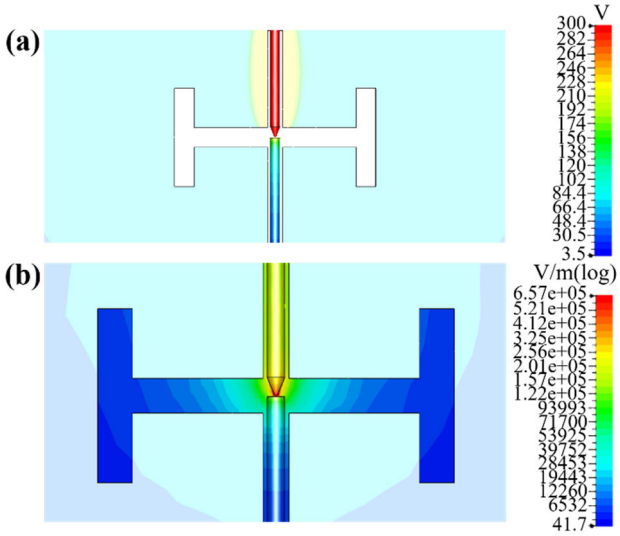

FIGURE 5. Simulated electrostatic model of an H-shaped slot structure; (a) Electrostatic potential, (b) Electrostatic field distribution.

body acts as a shield ring to suppress the electrostatic field concentration.

The experimental testbed for analyzing the effect of the electrostatic potential on the power limiter is shown in Fig. 6(a). The DC voltage source was connected to the upper and lower discharge electrodes. The coaxial waveguide adapter and cable were connected between the power limiter and the network analyzer to verify the effect of the electrostatic potential on the transfer characteristics. The cavity of plasma limiter was pumped to a pressure lower than 10E-1 torr, then it filled with a xenon gas at the correct pressure, and finally close a valve of the plasma limiter and turn off the pumping system. The power limiter was measured as shown in Fig. 7. Paschen's curves were extracted using various electrostatic potential values. The corona discharge was the lowest at a pressure of 20 Torr with a DC voltage of 425 V. As the pressure value moved

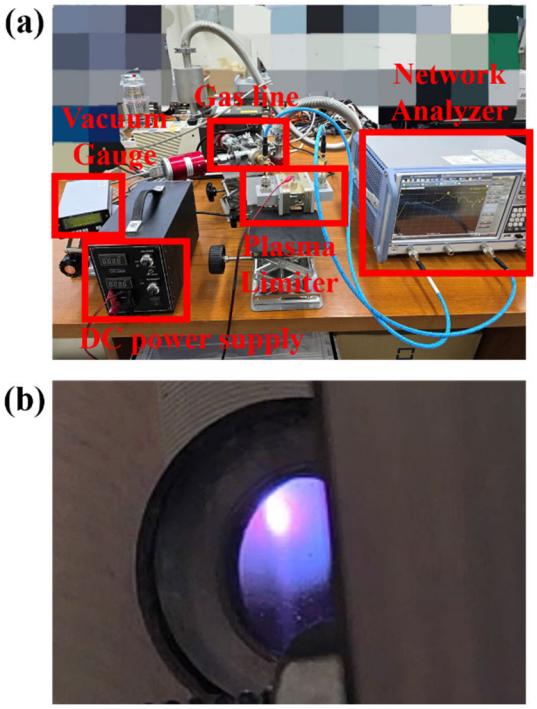

FIGURE 6. Photograph of experiments. (a) Test bed, (b) Electrostatic corona discharge.

away from the 20 Torr point, the electrostatic potential value required for the corona discharge increased. And the power consumption was less than 0.2 W and the current level was less than 2 mA. A photograph of the corona discharge is presented in Fig. 6(b). The corona discharge between the electrostatically biased electrodes has the characteristics of both streamer and glow discharges. In Fig. 7(b), a DC voltage of 414 V was electrically biased to the power limiter at a pressure of 20 Torr which is the point before the corona discharge. At a resonant frequency of 5.75 GHz, the insertion loss of the DC bias was 3.66 dB, which is an additional 1.81 dB loss compared with that of the nonbiased power limiter regarding with the pre-ionization effect. However, the plasma conductivity in the xenon gas was low, demonstrating an attenuation of 1.81 dB as shown in Fig. 7.

III. IMPULSE EXPERIMENTS AND RESULTS

Figure 8(a) shows a high-power electromagnetic impulse testbed of the waveguide type. The signal generator was utilized as the source signal, and the solid-state power amplifier was connected behind, which has a 42 dB gain in the frequency range of 5.4–5.9 GHz and a maximum output power of 1.2 kW. A waveguide-type circulator was installed at the front to protect the solid-state power amplifier from the reflected power of the power limiter. Directional couplers were installed at the front and back of the power limiter with a power meter to measure the incident, transmitted, and reflected powers in real time. A terminator was installed at

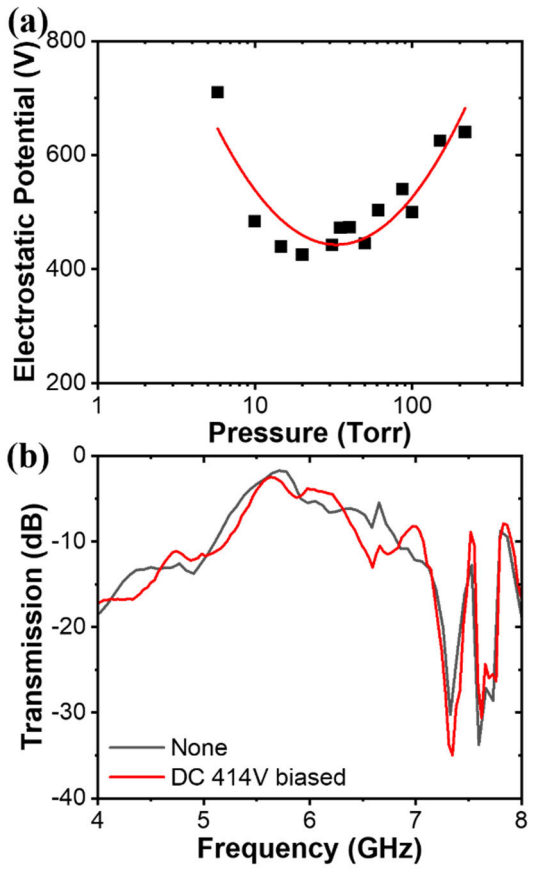

FIGURE 7. (a) Paschen's curve for various electrostatic potentials, (b) Transmission measurement results of the microwave power limiter with and without electrostatic potential bias.

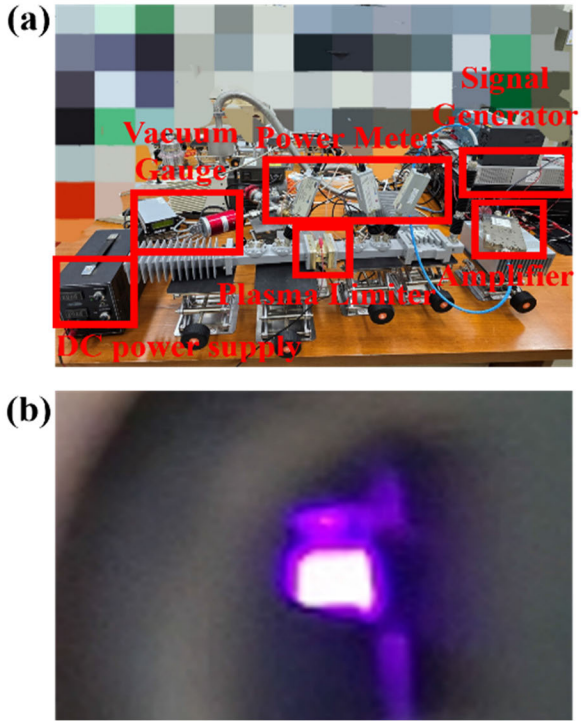

FIGURE 8. Photograph of impulse experiments; (a) Test bed, (b) Impulse corona discharge.

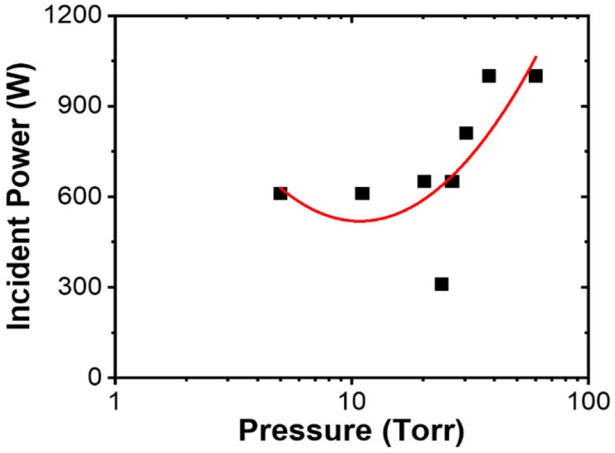

FIGURE 9. Paschen's curve for various incident powers.

the end of the test bed to absorb the transmitted high-power electromagnetic impulse. A 1 dB fixed attenuator was utilized in the stack and installed between the circulator and the solid-state power amplifier to control the incident power level. The rise time of the incident power was 20 ns, and the pulse width was 200 ns.

As shown in Fig. 9, the Paschen curve was extracted using various incident impulse power values, and the power limiter was filled with xenon gas. The plasma discharge was the lowest at a pressure of 24 Torr with an incident power of 310 W. As the pressure value moved away from 24 Torr, the incident power required for the plasma discharge increased. As the gap distance between the upper and lower discharging electrodes was 100 μm, modified paschen's curve is expected for the breakdown in microscale gaps [31]. The transfer characteristics of the power limiter are shown in Fig. 10, and were measured using a power meter in real time. When the power limiter was exposed to an impulse of 5.75 GHz with an incident power of 220 W, the transmitted power was 172 W, and the reflected power was 57 W, as shown in Fig. 10(a). The plasma limiter responded with a normal signal with minimal insertion loss as shown in Fig. 4. In Fig. 10(b), the incident, reflected, and transmitted powers are 332, 282, and 1.5 W, respectively. The response of the microwave power limiter to the plasma discharge is shown in Fig. 8(b). The transmitted power was suppressed, and most of the incident power was reflected. The plasma density is expected to have more than 10E17 m^{-3} which happens to make the incident wave to reflect [32].

Figure 11 shows the changes in the plasma discharge onset level at various electrostatic potentials. The microwave power limiter installed in the impulse test bed was connected to a DC voltage source. Without an electrostatic potential at the discharging electrode, the lowest onset level was 310 W,

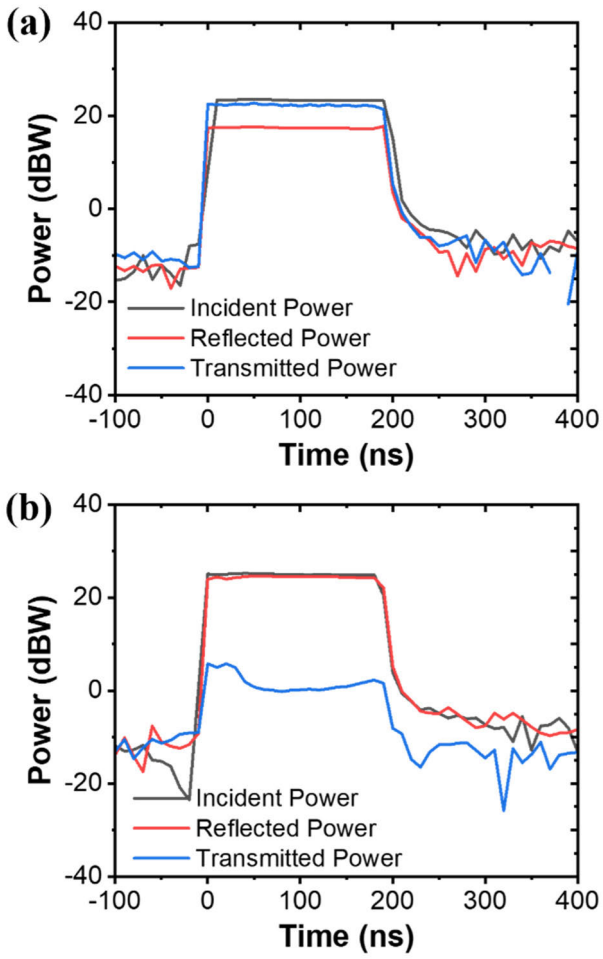

FIGURE 10. Impulse test result; Incident power of (a) 220 W and (b) 332 W.

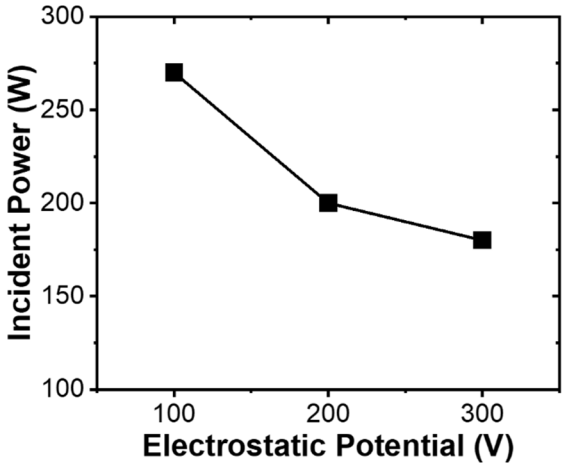

FIGURE 11. Change in the plasma discharge onset level by various electrostatic potentials.

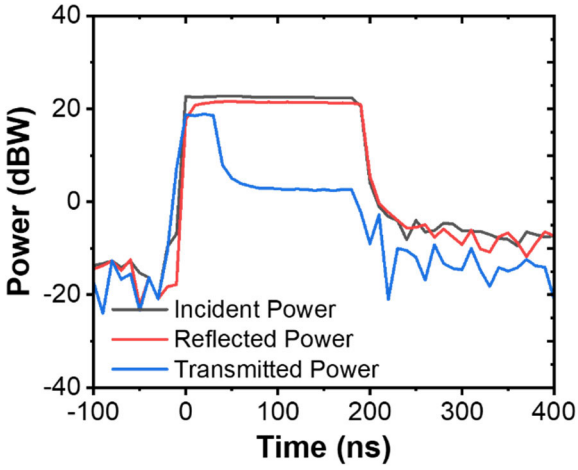

FIGURE 12. Impulse test result of power limiter with a DC bias of 300 V and an incident power of 180 W.

as shown in Fig. 9. With the DC bias of 100, 200, and 300 V, the incident powers of the plasma discharge onset level were 270, 200, and 180 W, respectively. Consequently, the plasma discharge onset level decreased with increasing electrostatic potential. Even when the electrostatic potential was biased to discharge the electrodes over 400 V, plasma discharge based on electrostatic field was observed. In Fig. 7(b), the bias of the electrostatic potential at the discharging electrode showed an attenuation of 1.81 dB; therefore, it is assumed that a small number of free electrons are discharged between the discharging electrodes in the xenon atmosphere, which helps lower the plasma discharge onset level. The transfer characteristics of the power limiter with the DC bias of 300 V are shown in Fig. 12. As the power limiter was exposed to an impulse of 5.75 GHz with an incident power of 180 W, the transmitted power was 2.1 W, and the reflected power was 142 W. The DC 300V biased power limiter has shown leakage power of 1.61 W, and 1.59 W for the incident power of 541 W and 1068 W, respectively. As the incident power leakage increases, the leakage power was reduced by enhancement of the plasma discharge. At the initial response time of 40 ns, the transmitted power was 77 W, whereas the unbiased power limiter showed a response time of 10 ns with suppressed leakage power, as shown in Fig. 10(b). And the response time was 10 ns and 20 ns for DC bias voltage of 100 V and 200 V, respectively. Therefore, when an electrostatic potential was applied to the power limiter, the plasma discharge onset level was decreased; however, the leakage power increased as the response time increased.

IV. CONCLUSION

The proposed microwave power limiter based on an H-shaped slot structure was demonstrated. The maximum electric field was 49492 V/m at the discharging electrode gap, which is 20% higher than that of the straight slot structure. The 3 dB bandwidths for the straight and H-shaped slot structures were compared in the simulation, and they were 952 and 708 MHz, respectively. The microwave power limiter demonstrated

an insertion loss of 1.85 dB at 5.75 GHz, and a 3 dB bandwidth at 535 MHz. To verify the effect of the electrostatic potential regarding with the pre-ionization, the calculated maximum electrostatic field in the gap between the discharge electrodes was 657 kV/m. In the electrostatic testbed, the corona discharged at the lowest pressure value of 20 Torr with DC 425 V. The transfer characteristics of the DC-biased power limiter showed an additional loss of 1.81 dB at a resonant frequency of 5.75 GHz. The microwave power limiter was tested using an impulse testbed with a high-power 5.75 GHz signal. Without the bias condition, the plasma discharged at the lowest pressure value of 24 Torr in the xenon atmosphere at an incident power of 310 W. By applying a DC voltage of 300 V, the plasma discharge onset level decreased to 180 W. In the time domain, the transmitted and reflected powers were 2.1 and 142 W, respectively. At the response time of 40 ns, the leakage power was 77 W. The power limiter has shown the operation result in a time domain, and the future plan is to measure the EMP suppression in a frequency domain. The proposed microwave power limiter exhibited an enhanced plasma discharge when an electrostatic potential was applied. Therefore, it is suitable for applications in RADAR systems for protecting LNAs from EMP threats. Furthermore, to suppress the leakage power during the response time, a diode limiter can be integrated to lower the response power of the microwave power limiter.

REFERENCES

[1] F. Liu, L. Zhou, C. Masouros, A. Li, W. Luo, and A. Petropulu, "Toward dual-functional radar-communication systems: Optimal waveform design," *IEEE Trans. Signal Process.*, vol. 66, no. 16, pp. 4264–4279, Aug. 2018.

[2] D. Long and F. Ulaby, *Microwave Radar and Radiometric Remote Sensing*. Norwood, MA, USA: Artech House, 2015.

[3] E. M. Staderini, "UWB radars in medicine," *IEEE Aerosp. Electron. Syst. Mag.*, vol. 17, no. 1, pp. 13–18, Jan. 2002.

[4] K. E. Olsen and W. Asen, "Bridging the gap between civilian and military passive radar," *IEEE Aerosp. Electron. Syst. Mag.*, vol. 32, no. 2, pp. 4–12, Feb. 2017.

[5] W. Wang, "Applications of MIMO technique for aerospace remote sensing," in *Proc. IEEE Aerosp. Conf.*, Big Sky, MT, USA, Feb. 2007, pp. 1–10.

[6] L. G. M. Prakasam, T. Roy, and D. Meena, "Digital signal generator and receiver design for S-band radar," in *Proc. IEEE Radar Conf.*, Waltham, MA, USA, Apr. 2007, pp. 1049–1054.

[7] E. Ragonese, G. Papotto, C. Nocera, A. Cavarra, and G. Palmisano, "CMOS automotive radar sensors: mm-wave circuit design challenges," *IEEE Trans. Circuits Syst. II, Exp. Briefs*, vol. 69, no. 6, pp. 2610–2616, Jun. 2022.

[8] D. Oliveira, N. Ghani, M. Hayat, J. Crichigno, and E. Bou-Harb, "SDN testbed for evaluation of large exo-atmospheric EMP attacks," *IEEE Commun. Mag.*, vol. 57, no. 1, pp. 88–97, Jan. 2019.

[9] S. A. S. Baharin, M. R. Ahmad, M. A. J. Akbar, and V. Cooray, "Electromagnetic interference from natural lightning on 4G communication links," *IEEE Access*, vol. 12, pp. 14870–14881, 2024.

[10] T. Kariya et al., "Development of over-MW gyrotrons for fusion at 14 GHz to sub-THz frequencies," *Nucl. Fusion*, vol. 57, no. 6, Jun. 2017, Art. no. 066001.

[11] S. K. Vyas, S. Maurya, R. K. Verma, and V. P. Singh, "Synthesis and simulation studies of a 10-kW 2.45-GHz CW magnetron," *IEEE Trans. Plasma Sci.*, vol. 43, no. 10, pp. 3615–3619, Oct. 2015.

[12] L. A. Samoska, "An overview of solid-state integrated circuit amplifiers in the submillimeter-wave and THz regime," *IEEE Trans. THz Sci. Technol.*, vol. 1, no. 1, pp. 9–24, Sep. 2011.

[13] J. Gut, "The Swiss EMP concept of general defense," *IEEE Antennas Propag. Soc. Newslett.*, vol. APSN-29, no. 6, pp. 4–10, Dec. 1987.

[14] J. Zhao, Q. Chen, G. Zhao, C. Chen, and Z. Chen, "Damage accumulation mechanism in PIN diode limiters induced via multiple microwave pulses," *Sci. Rep.*, vol. 10, no. 1, p. 1709, Feb. 2020.

[15] A. F. Miligy, Y. M. Madany, and A. M. Soliman, "Investigation and design of microwave receiver protector for meteorological radar applications," in *Proc. Int. Telecommun. Conf. (ITC-Egypt)*, Alexandria, Egypt, Jul. 2021, pp. 1–5.

[16] S. Yi and Z. Du, "The influence of microwave pulse repetition frequency on the thermal burnout effect of a PIN diode limiting-amplifying system," *Microelectron. Rel.*, vol. 85, pp. 156–162, Jun. 2018.

[17] S. Yi and Z. Du, "The influence of microwave pulse width on the thermal burnout effect of an LNA constructed by a GaAs PHEMT," *Microelectron. Rel.*, vol. 85, pp. 140–147, Jun. 2018.

[18] S. Yi and Z. Du, "Thermal burnout effect of a GaAs PHEMT LNA caused by repetitive microwave pulses," *IEEE Trans. Plasma Sci.*, vol. 47, no. 10, pp. 4620–4627, Oct. 2019.

[19] R. Zhao, X. Kang, Y. Zheng, H. Wu, N. Wei, S. Deng, K. Wei, and X. Liu, "High-power microwave limiters using recess-free AlGaN/GaN Schottky barrier diodes," *IEEE Microw. Wireless Technol. Lett.*, vol. 33, no. 2, pp. 208–211, Feb. 2023.

[20] J. Zhang, M. Lin, Z. Wu, L. Ding, L. Bian, and P. Liu, "Energy selective surface with power-dependent transmission coefficient for high-power microwave protection in waveguide," *IEEE Trans. Antennas Propag.*, vol. 67, no. 4, pp. 2494–2502, Apr. 2019.

[21] R. Phon and S. Lim, "Design and analysis of active metamaterial modulated by RF power level," *Sci. Rep.*, vol. 10, no. 1, p. 8703, May 2020.

[22] J. M. Woo, M. N. Ju, and J.-B. Lee, "Plasma-discharge-integrated slot structure for microwave power limiter," *Sci. Rep.*, vol. 13, no. 1, p. 10156, Jun. 2023.

[23] S. C. Gladson and M. Bhaskar, "A low power high-performance area efficient RF front-end exploiting body effect for 2.4 GHz IEEE 802.15.4 applications," *AEU-Int. J. Electron. Commun.*, vol. 96, pp. 81–92, Nov. 2018.

[24] M. S. Omran, S. Mirzanejhad, H. Zakeri-Khatir, and F. Sohbatzadeh, "Pressure and gas type effects on the plasma limiter operation at the S-band," *Brazilian J. Phys.*, vol. 52, no. 5, p. 165, Oct. 2022.

[25] Z. Zong and Y. Qiu, "Study on rapid response characteristics of plasma limiter under high power microwave," in *Proc. 7th Asia Int. Symp. Mechatronics*, vol. 588, 2020, pp. 95–106.

[26] B.-L. Zheng, S.-W. Wong, Y.-M. Wu, and Q.-X. Chu, "A novel stack PCB structure for X-band cavity bandpass filter implementation," in *Proc. Int. Appl. Comput. Electromagn. Soc. Symp. (ACES)*, Suzhou, China, Aug. 2017, pp. 1–2.

[27] H. Hu, X. Lei, and J. Wu, "Design of a compact dumbbell-shape twist waveguide with performance of band-pass filtering," in *Proc. IEEE 17th Int. Conf. Commun. Technol. (ICCT)*, Chengdu, China, Oct. 2017, pp. 1045–1048.

[28] F. Hu, H. Yi, and Z. Zhou, "Band-pass plasmonic slot filter with band selection and spectrally splitting capabilities," *Opt. Exp.*, vol. 19, no. 6, p. 4848, 2011.

[29] S. Nijdam, J. Teunissen, and U. Ebert, "The physics of streamer discharge phenomena," *Plasma Sources Sci. Technol.*, vol. 29, no. 10, Nov. 2020, Art. no. 103001.

[30] X. Cao, C. Li, H. Yan, Q. Hou, J. Dong, and W. Wang, "Key factors affecting the corona onset voltage of electrostatic precipitator electrodes," in *Proc. IEEE 16th Conf. Ind. Electron. Appl. (ICIEA)*, Chengdu, China, Aug. 2021, pp. 2119–2123.

[31] D. B. Go and D. A. Pohlman, "A mathematical model of the modified Paschen's curve for breakdown in microscale gaps," *J. Appl. Phys.*, vol. 107, no. 10, May 2010, Art. no. 103303.

[32] M. Magarotto, L. Schenato, M. Santagiustina, A. Galtarossa, and A.-D. Capobianco, "Plasma-based reflecting and transmitting surfaces," *IEEE Access*, vol. 11, pp. 91196–91205, 2023.

KYOUNG-JE PARK was born in Busan, South Korea, in 1991. He received the B.S. degree from the Department of Electronic Engineering, Silla University, South Korea, in 2016, and the M.S. degree in electronic engineering from Kyungpook National University, South Korea, in 2018. He is currently pursuing the Ph.D. degree with the Department of Electronic Engineering, Gyeongsang National University. His current research interest includes EMC/EMI/EMP analysis.

JAE-HYUN PARK received the B.S. degree from the Department of Electronic Engineering, Jeonbuk National University, South Korea, in 1991. He is currently the Director of the I-Spec Research Institute. His current research interest includes EMC/EMI/EMP analysis.

WANG-SANG LEE (Senior Member, IEEE) received the B.S. degree from Soongsil University, Seoul, South Korea, in 2004, and the M.S. and Ph.D. degrees in electrical engineering from Korea Advanced Institute of Science and Technology (KAIST), Daejeon, South Korea, in 2006 and 2013, respectively. Since 2014, he has been an Associate Professor with the Department of Electronic Engineering, Gyeongsang National University (GNU), Jinju, South Korea. His current research interests include near- and far-field wireless power and data communication systems, RF/microwave antennas, circuits and system design, RFID/the Internet of Things (IoT) sensors, and EMI/EMC.

JEONG-MIN WOO received the B.Sc. degree in electronics from Kyungpook National University, South Korea, in 2011, and the M.Sc. degree in information and communication engineering and the Ph.D. degree in electrical and electronic computer engineering from Gwangju Institute of Science and Technology, South Korea, in 2013 and 2016, respectively. He is currently a Senior Researcher with Korea Electrotechnology Research Institute. His current research interests include wireless power transfer, metamaterials, compound semiconductor devices, high-power electromagnetic pulse protection, analysis of HVDC electrical environmental effects, and static electric field sensors.